PEMIP: Post-fire Erosion Model Inter-comparison Project

Stephanie K. Kampf[a*], Benjamin M. Gannon[b], Codie Wilson[c], Freddy Saavedra[d], Mary Ellen Miller[e], Aaron Heldmyer[f], Ben Livneh[f,g], Peter Nelson[h], Lee MacDonald[i]

[a*]Corresponding author, Department of Ecosystem Science and Sustainability, Colorado State University, Fort Collins, CO 80523-1476, U.S.A. stephanie.kampf@colostate.edu. ORCID 0000-0001-8991-2679

[b]Colorado Forest Restoration Institute, Colorado State University, Fort Collins, CO 80523-1472, U.S.A. benjamin.gannon@colostate.edu

[c]Natural Resources Ecology Laboratory, 1499 Campus Delivery, Fort Collins, CO 80523-1499, USA. codie.wilson@colostate.edu

[d]Laboratorio de Teledetección Ambiental, Departamento de Ciencias Geográficas, Facultad de Ciencias Naturales y Exactas, Universidad de Playa Ancha, Valparaíso, Chile; HUB Ambiental UPLA, freddy.saavedra@upla.cl

[e]Michigan Tech Research Institute, Michigan Technical University, 3600 Green Court, Suite 100, Ann Arbor, MI 48105, USA. memiller@mtu.edu

[f]Department of Civil, Environmental, and Architectural Engineering, University of Colorado Boulder, USA. Aaron.Heldmyer@colorado.edu

[g]Cooperative Institute for Research in Environmental Sciences, University of Colorado Boulder, USA. Ben.Livneh@colorado.edu

[h]Department of Civil and Environmental Engineering, Colorado State University, 1372 Campus Delivery, Fort Collins, CO 80523-1372, USA. peter.nelson@colostate.edu

[i]Natural Resources Ecology Laboratory, 1499 Campus Delivery, Fort Collins, CO 80523-1499, USA. lee.macdonald@colostate.edu

Abstract

Land managers often need to predict watershed-scale erosion rates after disturbance or other land cover changes. This study compared commonly used hillslope erosion models to simulate post-fire sediment yields (SY) at both hillslope and watershed scales within the High Park Fire, Colorado, U.S.A. At hillslope scale, simulated SY from four models— RUSLE, AGWA/KINEROS2, WEPP, and a site-specific regression model—were compared to observed SY at 29 hillslopes. At the watershed scale, RUSLE, AGWA/KINEROS2, and WEPP were applied to simulate spatial patterns of SY for two 14-16 km^2 watersheds using different scales (0.5-25 ha) of hillslope discretization. Simulated spatial patterns were compared between models and to densities of channel heads across the watersheds. Three additional erosion algorithms were implemented within a land surface model to evaluate effects of parameter uncertainty. At the hillslope scale, SY was only significantly correlated to observed SY for the empirical model, but at the watershed scale, sediment loads were significantly correlated to observed channel head densities for all models. Watershed sediment load increased with the size of the hillslope sub-units due to the nonlinear effects of hillslope length on simulated erosion. SY's were closest in magnitude to expected watershed-scale SY when models were divided into the smallest hillslopes. These findings demonstrate that current erosion models are fairly consistent at identifying areas with low and high erosion potential, but the wide range of predicted SY and poor fit to observed SY highlight the need for better field observations and model calibration to obtain more accurate simulations.

Keywords: Erosion model, Hillslope scale, Watershed scale, WEPP, RUSLE, KINEROS2

Highlights

- Evaluated performance of erosion models at hillslope and watershed scales
- Simulated hillslope sediment yields did not correlate with measured values
- Simulated watershed sediment yields were correlated with observed rill densities
- Longer hillslopes within watershed simulations led to greater sediment loads
- Parameter uncertainty caused >2 orders of magnitude variability in sediment yields

1. Introduction

Soil erosion is a common problem in disturbed landscapes that has motivated the development of many models to help land and water managers predict erosion magnitudes and examine causes of variability in erosion rates (Merritt et al., 2003; Aksoy and Kavvas, 2005). Erosion models can be used to evaluate how management actions or disturbances affect soil loss, sedimentation, and/or water quality degradation. Models can also be applied to estimate spatial patterns of erosion, identify areas where land use changes such as timber harvest or road construction should be restricted, and determine where erosion mitigation would be most beneficial after large disturbances like wildfire (Miller et al. 2016). Most erosion models have been developed for agricultural areas using data collected from small plots or hillslopes (Wischmeier and Smith, 1965; Flanagan and Nearing, 1995), but they are often applied to predict erosion over large watersheds with diverse topography, soils, and land cover (e.g., Millward and Mersey, 1999; Fu et al., 2005; Baigorria and Romero, 2007; Shen et al., 2009). Evaluations of erosion model performance at the watershed scale are limited, making it difficult for land and water managers to identify which erosion model is most appropriate for their local conditions and scales of analysis.

Erosion models for land management have varying computational approaches. In the U.S., two common erosion models are the Watershed Erosion Prediction Project (WEPP) (Flanagan and Nearing, 1995) and the kinematic runoff and erosion model (KINEROS2) (Smith et al., 1995), both of which have been adapted for post-fire applications. Both are physically-based erosion models with long histories of code development. The empirical Revised Universal Soil Loss Equation (RUSLE) (Renard et al., 1997) is perhaps the most frequently applied erosion model, and it is often integrated into decision support tools (Sharp et al. 2018; Gannon et al. 2019). Hydrologic models are becoming increasingly modularized, which facilitates integration of different types of erosion simulation modules (Ahuja et al., 2005; Stewart et al., 2017). Yet, even as erosion model types have proliferated, measurements to evaluate their performance remain sparse.

In this paper we evaluate the performance of erosion models at multiple scales of analysis and offer guidance about selecting models for erosion simulation. We conducted this model analysis for two 14-16 km^2 burned watersheds with specific objectives to: (1) evaluate the performance of the models for simulating hillslope erosion; (2) compare total magnitudes and

spatial patterns of simulated erosion across watersheds divided into varying sizes of hillslopes; (3) quantify potential effects of parameter uncertainty on simulated watershed-scale erosion, and (4) evaluate the relative accuracy of models at the watershed scale using a combination of quantitative and qualitative observations of surface erosion.

2. Background

2.1. Erosion models

One of the oldest and most widely used erosion models is the Universal Soil Loss Equation (USLE) (Wischmeir and Smith, 1965). This empirical model was developed from small plot data collected at research sites across the U.S. Most plots were 2 m (6 ft) wide by 22 m (72 ft) long, and slopes matched the local terrain (Laflen and Flanagan, 2013). USLE predicts annual total erosion as a function of rainfall erosivity, soil erodibility, length, slope, cover, and erosion control practices. Modifications to the length-slope and cover factors resulted in the Revised Universal Soil Loss Equation (RUSLE) (Renard et al., 1997). Many models incorporate some version of USLE to simulate erosion (Laflen and Flanagan, 2013). One of these, the Modified Universal Soil Loss Equation (MUSLE), replaced rainfall erosivity with storm runoff volume and peak runoff rate to predict erosion from individual storms (Williams, 1975; Williams and Berndt, 1977). USLE and its variants are easily integrated with other models because the equations all have analytical solutions. While USLE was designed for individual hillslope use, gridded versions have also been developed to predict erosion across large areas (Theobald et al., 2010; Lischert et al., 2014; Yochum and Norman, 2014).

Although easy to implement, USLE and its variants are not well-suited to predict changing erosion conditions over time because they do not represent time varying soil moisture and infiltration. To simulate these time varying processes and their effects on erosion, researchers at the USDA Agricultural Research Service (ARS) developed the Water Erosion Prediction Project (WEPP) (Flanagan and Nearing, 1995). The project used the field data collected for USLE as well as additional field experiments conducted on 9-11 m (30-36 ft) long and 0.5-3 m (2-10 ft) plots (Laflen et al., 1991). The resulting WEPP model simulates erosion and deposition within hillslopes as functions of rainfall input during storms, overland flow generation, detachment of sediment by overland flow in rill and inter-rill areas, and flow competency to transport sediment (Flanagan and Nearing, 1995). WEPP can use historical

climate data to represent actual storms, but typically simulations are run for many stochastic weather scenarios (≥ 50). Each hillslope can be decomposed into multiple overland flow elements (sections) with different slopes. WEPP can also account for plant growth and residue decomposition, evapotranspiration, deep percolation and subsurface lateral flows (Dun et al., 2009; Srivastava, 2013). WEPP consists of two versions: a hillslope version to estimate the distribution of erosion on a hillslope and a watershed version that links hillslopes with channels and in-stream structures to estimate sediment delivery from small watersheds. Multiple standalone and online modelling interfaces are available for parameterizing and running WEPP (Miller et al., 2017; Frankenberger et al., 2011; Benda et al. 2007; Elliot, 2004; Renschler, 2003).

Separate from the development of WEPP, scientists at the USDA-ARS developed KINEROS2, the KINEmatic runoff and EROSion model (Woolhiser et al., 1990; Smith et al., 1995). KINEROS2 is a physically-based model that simulates both rain splash erosion as a function of rain rate and hydraulic erosion as a function of overland flow rate. KINEROS2 predicts erosion for rectangular planes, which are connected by channels for watershed-scale modeling (Goodrich et al., 2012). Planes in KINEROS2 can be assigned a single slope or divided into multiple segments. Sediment outputs are represented by distributions of up to five particle size classes. The model is designed to simulate single rainfall-runoff events rather than long-term erosion. To facilitate application over larger areas, the Automated Geospatial Watershed Assessment tool (AGWA) can be used to discretize hillslopes and compile parameters for running KINEROS2 in the ArcGIS environment (Miller et al., 2007). Field studies to guide parameter estimation have not been conducted for the erosion submodels in KINEROS2, so this model has not been as widely applied as the WEPP model.

Erosion modules have also been added to other hydrologic models originally designed for streamflow simulation. For example, Stewart et al. (2017) incorporated multiple erosion modules into the Variable Infiltration Capacity (VIC) model, which simulates land surface processes and streamflow generation for large river basins (Liang et al., 1994). This single unified framework standardizes the sediment model inputs and VIC boundary conditions to facilitate consistent comparison across simulations that apply different erosion modules. The erosion modules incorporated into VIC include MUSLE, the Hydrologic Simulation Program Fortran (HSPF), and the Distributed Hydrology Soil Vegetation Model (DHSVM). HSPF (Johnson and Davis, 1980; Bicknell et al., 1996) was initially developed by the U.S. Environmental Protection Agency to

simulate contaminant transport, and it represents surface runoff generation using a conceptual approach. DHSVM (Wigmosta et al., 1994) uses the erosion simulation approach from the Systeme Hydrologique European – Sediment (SHE-SED) model (Wicks and Bathurst, 1996) to compute sediment detachment and transport for individual elements (analogous to hillslopes) connected by stream reaches. DHSVM simulates overland flow for individual grid cells, connected to each other via topographic routing, and detached sediment is transported as suspended sediment based on the transport capacity of overland flow (Doten et al., 2006).

2.2. Post-fire applications

Many of the models described in the previous section have been applied to simulate post-fire erosion. These applications involve changing model parameters to represent post-fire conditions; for instance, decreasing ground cover, reducing soil infiltration capacity, increasing soil erodibility, decreasing surface roughness, and decreasing root cohesion (Miller et al., 2003; Elliott, 2004; Canfield and Goodrich, 2005; Doten et al., 2006; Robichaud et al., 2007; Larsen and MacDonald, 2007; Miller et al., 2012; Miller et al., 2016; Elliott et al., 2016; Robichaud et al., 2016; Jones et al. 2017; Srivastava et al., 2018; Gannon et al., 2019). Given the limited availability of post-fire erosion data, most erosion modeling studies do not compare simulated erosion to observations. Of the studies that do incorporate observations, simulated erosion rates are not well-correlated to individual hillslope observations, but models tend to perform better when hillslopes are grouped (Larsen and MacDonald, 2007; Miller et al., 2012) or when relative ranks of erosion rates are compared between simulations and observations (Robichaud et al. 2016). Empirical regression models for predicting post-fire erosion have been developed for specific study areas (Benavides-Solorio and MacDonald, 2005; Schmeer et al., 2018), and these tend to have stronger performance than the process-based erosion models. However, the models do not perform as well when applied to new areas not used in model development (Schmeer et al., 2018), and regression models do not represent physical processes directly.

Prior model-observation comparisons have been conducted at the hillslope scale, where erosion is caused by overland flow. How well these models perform at watershed scale remains largely unknown. Sediment yields tend to decline with greater drainage area due to deposition along flow paths, but these scaling relationships have substantial variability (Wagenbrenner and Robichaud, 2014). The few studies that have evaluated stream sediment yields after fire have used only suspended sediment (e.g. Kunze and Stednick, 2006; Desilets et al., 2007), which may

lead to inaccurate sediment yield predictions when there is substantial bedload transport and/or deposition. Post-fire streams can have rapid and frequent changes in channel geometry (e.g. Brogan et al., 2019a,b; Wilson 2019), so accurate sediment yield measurement would require continuously monitoring suspended sediment, bed load, changes in channel geometry at the watershed outlet, and a method for deriving accurate streamflow. Given the cost and labor required for such measurements, observations of post-fire erosion at the watershed scale remain limited.

3. Methods

3.1. Study area

We focused our analysis on two watersheds that burned in the 2012 High Park Fire in northern Colorado to make use of previous field observations for model evaluation (Kampf et al., 2016; Schmeer et al., 2018; Brogan et al., 2019b). This fire burned over 350 km^2 of primarily forested land. Researchers conducted post-fire erosion and channel monitoring within two ~14-16 km^2 watersheds called Skin Gulch and Hill Gulch (Figure 1). These watersheds were burned at moderate to high severity over 65-70% of their area (Brogan et al., 2019b; Schmeer et al., 2018) and range in elevation from 1740-2580 m. Prior to the fire, land cover was primarily ponderosa pine (*Pinus ponderosa*) woodland and forest with some shrublands and grasslands at lower elevations and mixed conifer forest at higher elevations. The climate is semiarid, with mean annual precipitation between 440-600 mm (PRISM Climate Group). Soils are mostly shallow sandy loams, and bedrock outcrops are common on steep slopes.

Erosion rates were measured from late 2012-2015 at 29 sediment fences that captured the sediment eroded from convergent hillslopes. The mass of sediment collected in each sediment fence was measured in the field, converted to dry mass, and normalized by hillslope drainage area to give sediment yields (SY). Drainage areas of these hillslopes ranged from 0.1-1.5 ha, with slopes from 11-65% and lengths from 48-270 m. Eight of the hillslopes were mulched with straw or wood chips after the fire to reduce erosion. The hillslopes were installed in clusters of four to seven sites in the upper, middle, and lower elevations of the study watersheds, with each cluster containing at least one tipping bucket rain gauge (details in Schmeer et al. 2018). This paper focuses on modeling the total erosion during a sequence of rain storms in summer 2013,

215 which included 12 convective thunderstorms in July and August and one large long-duration
216 storm in September that produced more than 250 mm of rainfall (Kampf et al., 2016). We
217 selected the time period from June-October 2013 for our analysis because the majority of the
218 post-fire erosion measured at these sites was produced in this time frame.

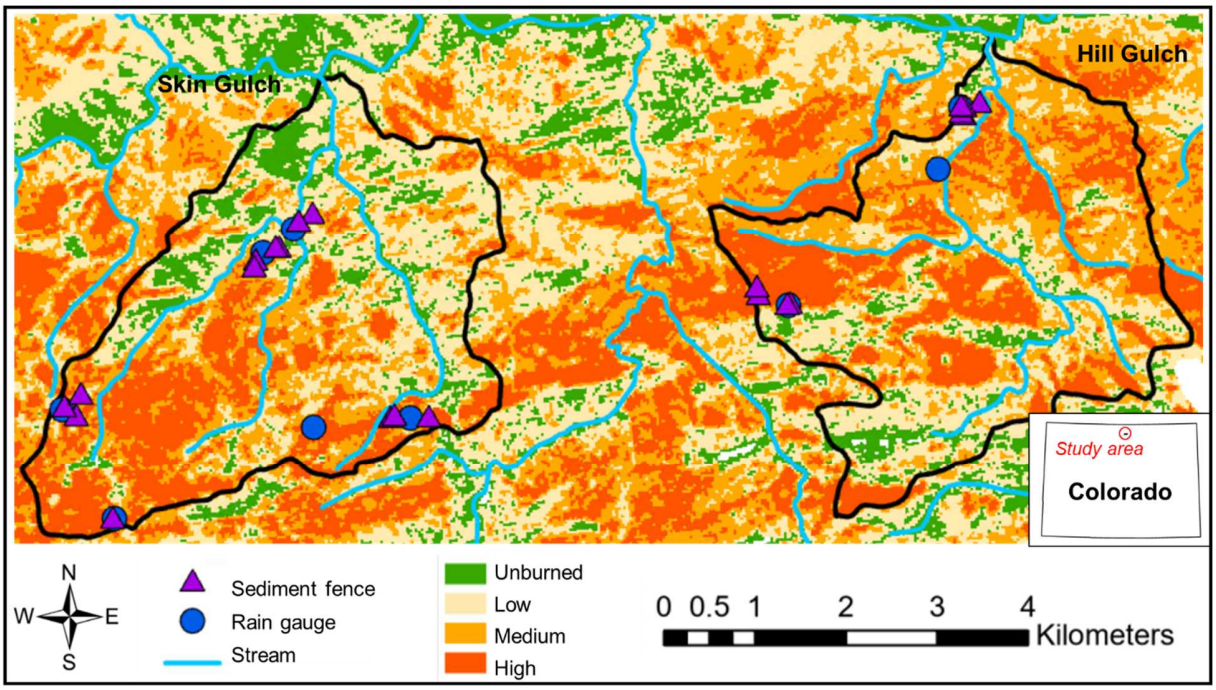

219

220 **Fig. 1** Study watersheds, Skin Gulch and Hill Gulch, overlying the Monitoring Trends in Burn
221 Severity (MTBS) burn severity map for the 2012 High Park Fire in Colorado. Locations
222 of field measurements for rainfall (rain gauges) and sediment yield (sediment fences) also
223 shown

224

225 ### 3.2. Model applications

226 We applied four models to simulate seasonal total SY at the hillslope scale: the regression
227 model of Schmeer et al. (2018), RUSLE, WEPP, and AGWA/KINEROS2. Each model is
228 described in detail in the following sections. Hillslope-scale models were each evaluated using
229 correlation analyses and comparisons of summary statistics between simulated and observed
230 hillslope SY. We then applied RUSLE, WEPP, and AGWA-KINEROS2 to simulate watershed-
231 scale SY for each of the two study watersheds with varying sizes of hillslope sub-units to
232 examine which models and sizes of hillslope sub-units best approximate the observed spatial
233 patterns of erosion and expected watershed SY. Finally, to evaluate how parameter uncertainty

affects watershed-scale simulations, we created ensembles of possible watershed-scale erosion rates using the erosion modules within VIC. Each of these steps is described in detail below.

3.2.1. Empirical model

The empirical model from Schmeer et al. (2018) was developed for the hillslope scale using the observed hillslope characteristics and SY. The model equation is:

$$SY = K_1 + K_2 \times (P^{\alpha} \times B^{\beta} \times L^{\gamma}) + \varepsilon \quad (1)$$

where SY is the sediment yield (Mg ha^{-1}); K_1 is an additive shift that adjusts for overall bias in the empirical model (Equation 1 of Schmeer et al., 2018); P is the depth (mm) of rainfall from June-Sept.; B is the percent of bare soil (%B), and L is the maximum flow length (m) of each hillslope. The powers (α, β, and γ) and the empirical coefficient (K_2) were identified by Schmeer et al. (2018) as those that minimized average prediction error (ε): K_1 = -0.05, K_2*1000 = 5.6, α = 1.1, β = 1.5, γ = -1.1, ε = 3.7.

We ran this model for the observed hillslopes using two different sets of input: (1) field observations, and (2) values derived from spatial datasets; these spatial dataset values are needed to apply models at the watershed scale. Both model runs used field values of P from the nearest rain gauge to each hillslope. The field values of %B are from field ground cover measurements, which were point counts along transects (Schmeer et al., 2018). Derived values of %B were assigned based on burn severity classes from the Monitoring Trends in Burn Severity (MTBS) map (Eidenshink et al., 2007) and the default cover values in Disturbed WEPP for forest, and low to high severity fire (Elliot, 2004). Unburned areas were assigned bare soil values of 0%; low severity fire 15%; moderate severity fire 35%, and high severity fire 55%. We assigned the average observed mulch cover for spring 2013 (38%) to all mulched hillslopes. Field observations of L came from Schmeer et al. (2018), and derived values of L were determined using the hillslope delineation tool in AGWA.

3.2.2. RUSLE

The RUSLE model is a hillslope-scale model, but it can be applied at watershed scale by dividing watersheds up into hillslopes and summing the total erosion. RUSLE applies the equation:

$$A = RKLSCP \quad (2)$$

where A is the soil erosion rate (Mg ha^{-1} hr^{-1}); R is the rainfall erosivity (EI_{30}); K is the soil erodibility; L is the length factor; S is the slope factor; C is the cover factor; P is the erosion control practice factor.

For R we used the closest rain gauge to each hillslope to compute EI_{30} from June-October 2013. For soil erodibility we used the whole soil K factor from the Soil Survey Geographic Database (SSURGO), which is a soil database with soil units mapped at scales of 1:12,000 to 1:63,360 (Soil Survey Staff, 2014). We used the coarser 1:250,000 State Soils Geographic Database (STATSGO) for areas where SSURGO data did not include K factor values. Each hillslope was assigned the K value from the soil survey polygon covering the largest total area in the hillslope. We followed the methods of Yochum and Norman (2015) to calculate the K factor for all components within each soil map unit as the depth-weighted mean for the top 15 cm of soil for each component, and as the area-weighted mean for any non-water or non-rock components of the map unit. K was converted to metric units (Mg ha hr ha^{-1} MJ^{-1} mm^{-1}) according to Renard et al. (1997). K was adjusted for post-fire conditions using multiplication factors to increase the K for different levels of burn severity: 1.5 for low severity; 1.75 for moderate severity, and 2.0 for high severity (Schmeer, 2014).

L is the length factor, defined as:

$$L = \left(\frac{\lambda}{22.13}\right)^{m} \quad (3)$$

where λ is the slope length (m), and *m* is an exponent related to the ratio of rill to interrill erosion, expressed as:

$$m = \frac{\beta}{1+\beta} \quad (4)$$

where β is expressed as:

$$\beta = {(\sin\theta/0.0896)}\Big/{[3.0\ (\sin\theta)^{0.8} + 0.56]} \quad (5)$$

and θ is the slope angle in radians.

The slope factor, S, for soils with primarily surface flow and high susceptibility to erosion is defined as

$$S = 10.8 \sin\theta + 0.03 \quad (6)$$

295 for slopes < 9%, and as

296 $$S = (\sin\theta / 0.0896)^{0.6} \quad (7)$$

297 for slopes ≥ 9%, where θ is the slope angle in radians.

298 C is the cover factor, which we assigned based on mean field measurements by burn
299 severity from Larsen and MacDonald (2007); low, moderate, and high burn severity were
300 assigned C factors of 0.01, 0.05, and 0.20 respectively. Finally, P is the support practice factor,
301 which is used to represent mulch. Areas with >50% straw or wood shred mulch were assigned a
302 value of 0.22 (Schmeer 2014). All other areas were assigned a P factor of 1.
303

304 ### 3.2.3. WEPP and AGWA-KINEROS2

305 WEPP and AGWA-KINEROS2 were applied both for the observed hillslope simulations
306 and for the watershed-scale simulations. Contributing areas for each hillslope were delineated for
307 WEPP Watershed using WEPP's delineation tool, the Topographic Parameterization (TOPAZ)
308 (Garbrecht and Martz, 1997), and for KINEROS2 using AGWA. Precipitation input was
309 assigned using the nearest tipping bucket rain gauge (Figure 1). WEPP requires additional
310 atmospheric variables: temperature, solar radiation, dew point, wind speed, and wind direction.
311 Values were compiled from the Red Feather Lakes Remote Automated Weather Station
312 (RAWS), which is about 20 km NW of the study watersheds; although these atmospheric
313 variables are required by WEPP they have limited influence on erosion rates. KINEROS2
314 requires initial soil moisture values prior to each event; because we did not have soil moisture
315 measurements we set these to the default value of 0.2. Soil parameters required by the models
316 include saturated hydraulic conductivity, particle sizes as percent sand, silt, and clay, rock
317 content, and porosity. These values were taken from SSURGO and STATSGO as described in
318 section 3.2.2. Land cover parameters required by the models include percent cover, interception
319 storage, and surface roughness. These were taken from the Existing Vegetation Type (EVT)
320 developed by the LANDFIRE program using decision tree models, field data, Landsat imagery,
321 elevation, and biophysical gradient data combined with the soil burn severity map to change land
322 cover parameters for each burn severity class (Elliott, 2004; Canfield and Goodrich, 2005;
323 Robichaud et al., 2007). Both WEPP and AGWA have built-in approaches for assigning soil and
324 vegetation parameters and for modifying parameters based on burn severity class. We did not

calibrate the models because we were interested in how these tools perform for management applications, where erosion observations are not available.

3.2.4. Watershed-scale simulations

Watershed-scale sediment loads are often estimated by summing the sediment loads of all hillslopes within the watershed, which are sensitive to the size of the hillslope sub-units. To understand the influence of hillslope size, we developed a range of watershed-scale simulations by dividing up the watersheds into hillslopes with different target sizes: 0.5, 1, 2.5, 5, 10, 15, and 25 ha using a 10 m digital elevation model. This range of sizes was based on the ability of TOPAZ to define hillslopes at different resolutions; TOPAZ failed when the target hillslope size was smaller or larger than this range. We then used the hillslope delineation algorithm within AGWA to create hillslopes with the same set of target areas for AGWA-KINEROS2. The hillslope delineations are similar but not exactly the same for WEPP and AGWA-KINEROS2, except at 25 ha target areas. Precipitation inputs and parameter values for each model came from the same sources described for the hillslope simulations. In addition to the simulations for hillslopes of different sizes, we applied a gridded version of RUSLE to 30 m raster cells across each watershed (Winchell et al., 2008; Gannon et al. 2019); this comparison was added because gridded RUSLE has become a popular approach for erosion modeling.

To evaluate effects of parameter uncertainty on watershed-scale sediment yields we used the erosion modules in VIC (i.e., MUSLE, HSPF, DHSVM). Each module was run for all ranges of hillslope sizes using variable plausible parameter values. Initial parameter settings were based on Livneh et al. (2013; 2015) and Stewart et al. (2017), who applied the VIC erosion modules to simulations for this region. VIC vegetation settings were adjusted to account for wildfire effects using the same percent cover estimates generated for each hillslope in AGWA-KINEROS2. Parameters that most affected erosion rates were identified for each erosion module using a Sobol sensitivity analysis. This led to selection of eight VIC soil parameters, which were varied using bounds from published studies (Demaria et al., 2007; Troy et al., 2008; Yanto et al., 2017), as well as nine suspended sediment loading (SSL) parameters, which were varied using bounds from Doten et al. (2006), Maidment (1993), and Donigian and Love (2003).

To evaluate the spatial patterns of simulated erosion within watersheds we compared simulated erosion rates to the density of channel heads. The channel density in the study area

356 increased dramatically after the fire due to post-fire erosion (Henkle et al., 2011; Wohl 2013).
357 We visually identified locations of channel heads at the tops of rills or gullies (Figure 2) from
358 National Ecological Observatory Network (NEON) aerial camera images with 25 cm resolution
359 for June 28-July 16, 2013 and Larimer County 0.2 m resolution imagery obtained from
360 Pictometry for September 1, 2012. Rills and gullies were distinguishable from the main stream
361 channels because the larger streams typically still retained some riparian vegetation. We
362 computed the fraction of watershed total channel heads within each of the 25 ha hillslopes and
363 evaluated the correlations of these values with fractions of total simulated sediment load
364 predicted in the models. The channel head density is a reasonable surrogate for relative erosion
365 rates across the watersheds, as it was infeasible to measure absolute erosion rates for sub-
366 watersheds larger than 1.5 ha.

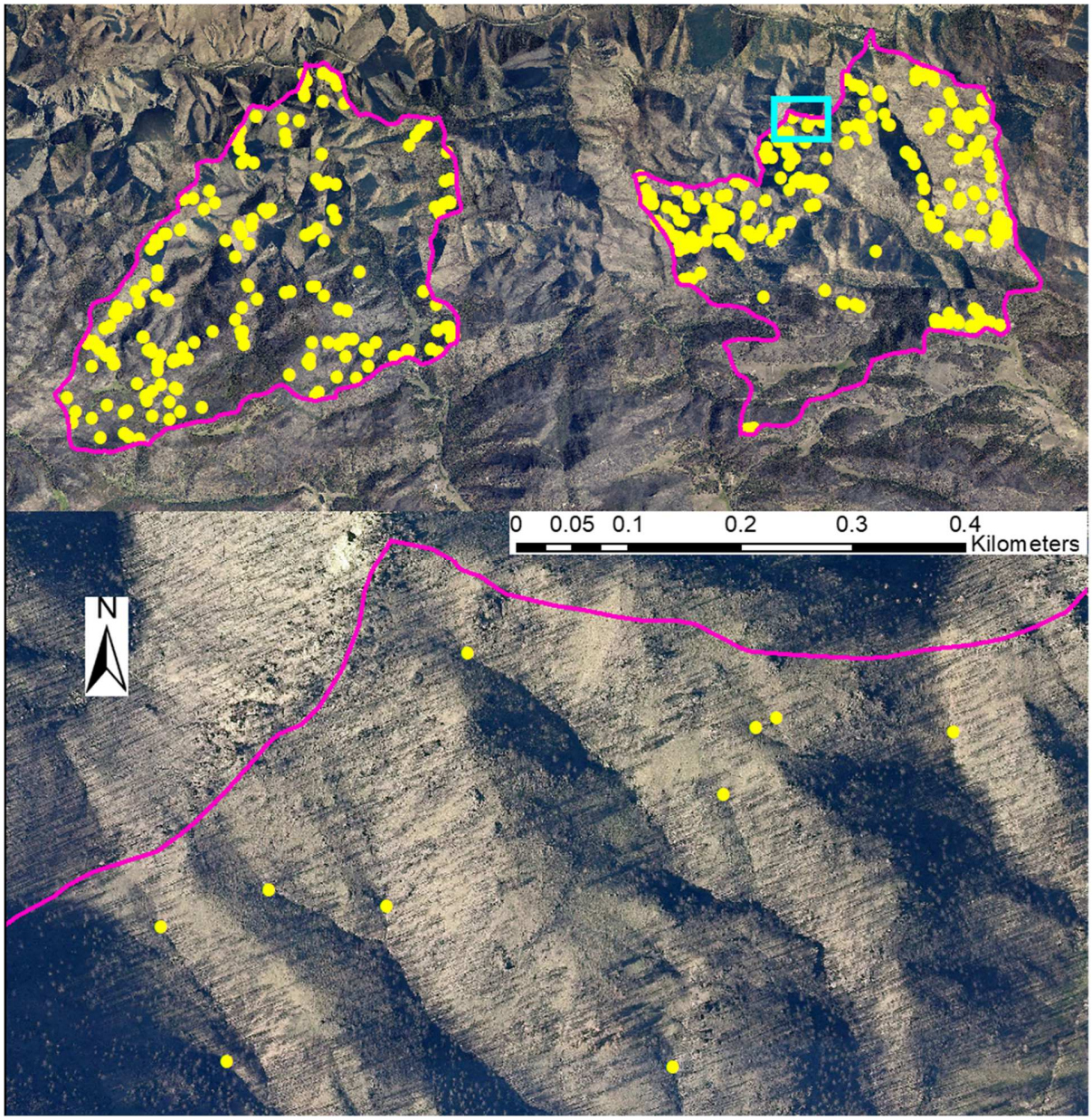

Fig. 2 Visual evidence of surface erosion in 2012 Pictometry air photos. Top image shows locations of digitized channel heads (yellow) in Skin Gulch (left) and Hill Gulch (right), and bottom image zooms into the boxed area in Hill Gulch

We then compared total watershed-scale sediment load (SL, Mg) and SY (Mg ha^{-1}) for both study watersheds, each model (RUSLE, WEPP, AGWA-KINEROS2, and the VIC modules), and each size of hillslope sub-units. For the models designed for spatial application (RUSLE, WEPP, AGWA-KINEROS2), we also evaluated how the fraction of watershed total

SL for each hillslope varied between each of the models using Pearson and Spearman correlation analysis. We used fractions of total sediment load rather than actual SL values because magnitudes of SL varied substantially between models.

4. Results

4.1. Hillslope scale

When compared to sediment yields measured at sediment fences, most of the models did not perform well. Only the empirical regression model was significantly correlated to observed seasonal total sediment yields (SY) when the original field measurements were used as inputs (Table 1, Figure 3a). When the regression model was applied using inputs from geospatial datasets, predictions of SY were not significantly correlated with observed SY (Figure 3b), primarily because the estimated percent bare soil using burn severity and mulch locations had no correlation to the observed percent bare soil (R^2=0.03). This indicates that one major source of error in models applied to unmonitored areas is the accuracy of the geospatial datasets used to parameterize the models.

RUSLE mostly under-predicted SY, but five sites in Skin Gulch had predicted SY values that were much higher than observed (Figure 3c); these over-predicted sites all had long slopes (>150 m). AGWA-KINEROS2 over-predicted SY for many of the Skin Gulch hillslopes and under-predicted SY for the un-mulched Hill Gulch hillslopes (Figure 3d). The range of SY predicted by WEPP was consistent with the observed range of SY, but the predicted values had no correlation with the observed values (Table 1; Figure 3e,f). Hillslope SY observations are often biased low because sediment fences can fill to capacity with sediment, and suspended sediment can bypass the collection fence (Wilson 2019). However, we did not identify any connection between under- or over-prediction of simulated SY and the locations where the sediment fences had over-topped with sediment.

Because of the lack of correlations between simulated and observed SY, we also compared the means and standard deviations of SY between observations and models. The empirical model with field-derived inputs and the WEPP model both produced mean SY values that were within 15% of the observed values (Table 1). RUSLE and AGWA-KINEROS2 over-predicted the mean and standard deviations of SY by factors of three or more, whereas the empirical model with derived inputs predicted only about half of the measured SY.

407 **Table 1**. Summary of model performance for simulating sediment yields compared to the
408 observed hillslope values. Asterisks indicate significant at $p<0.05$. Table also indicates the mean
409 and standard deviation of sediment yield (Mg ha^{-1}) for both the observed and simulated values;
410 RMSE also in (Mg ha^{-1}).

Model	**R^2**	**RMSE**	**Intercept**	**Slope**	**Mean**	**Std Dev**
Observed					11.2	10.1
Empirical, field inputs	0.60*	5.2	3.4*	0.61*	10.2	8.0
Empirical, derived inputs	0.13	2.7	4.7*	0.10	5.8	2.9
RUSLE	0.04	23.2	13.6*	-0.44	61.5	102.8
AGWA-KINEROS2	0.07	43.0	42.9*	-1.13	30.3	43.7
WEPP	0.00	10.3	10.4*	0.05	12.7	10.9

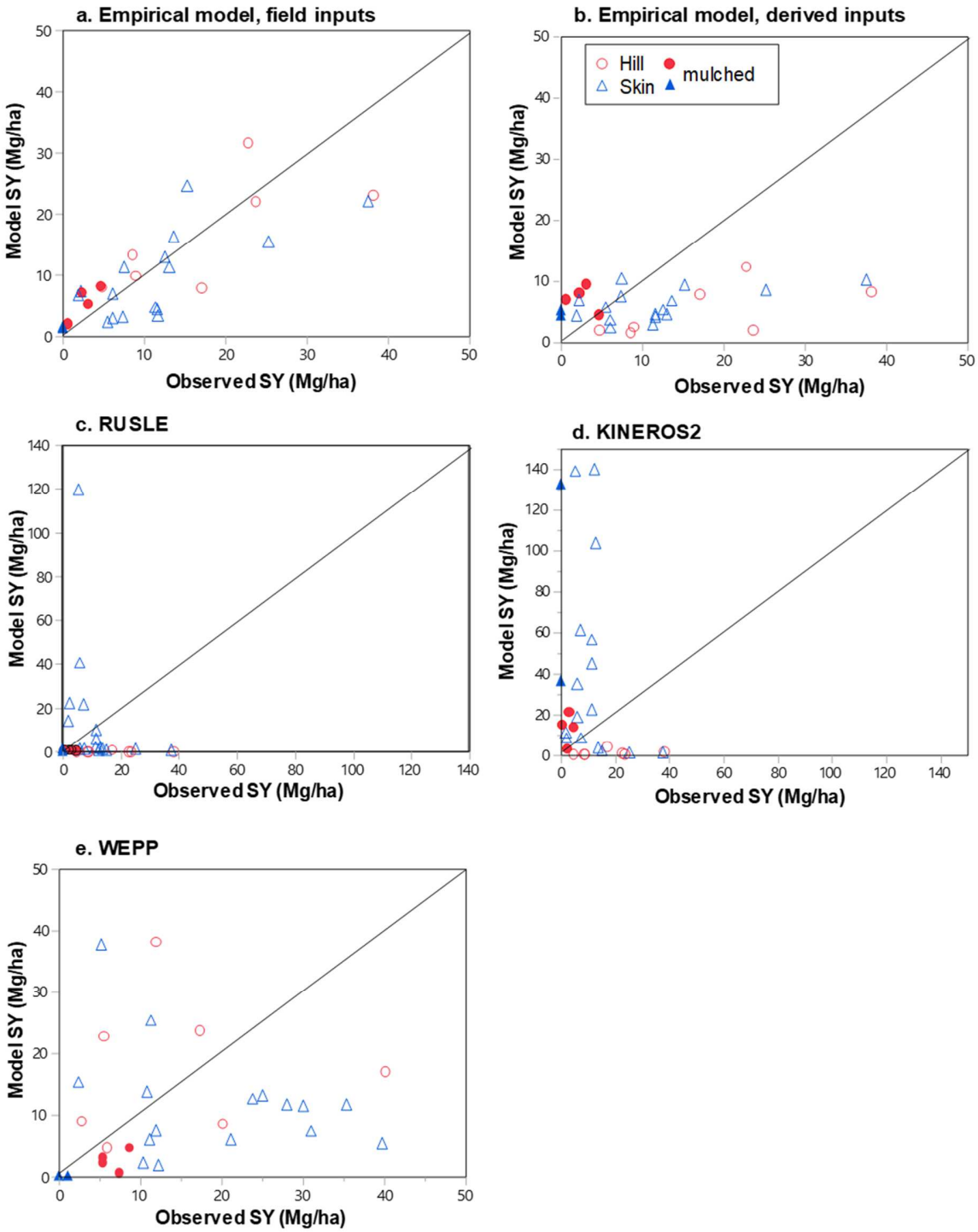

411

412 **Fig. 3** Simulated total sediment yield (SY) for June-October 2013 compared to observed SY at
413 hillslopes from (a) Schmeer et al. (2018) empirical model with inputs from field
414 measurements; (b) same as (a) except with inputs derived from geospatial data; (c)
415 RUSLE; (d) AGWA-KINEROS2; (e) WEPP. Line is 1:1. Data in Kampf et al (2020).

4.2. Watershed scale

Each of the models produced different magnitudes and spatial patterns of seasonal total SY across the study watersheds. The ranges of watershed total SL (and SY) varied from $9x10^3$ Mg (6 Mg ha^{-1}) in WEPP to $2x10^6$ Mg (2000 Mg ha^{-1}) in VIC-MUSLE, with values varying between models and with the size of hillslopes within each simulation (Table 2). In comparison, observed hillslopes had a mean SY of 11 Mg ha^{-1} and maximum of 38 Mg ha^{-1}, which converts to $2x10^4$ - $4x10^4$ Mg per watershed if the mean value is applied uniformly. Uncertainties in these watershed-scale estimates stem from variability in hillslope characteristics and burn severity, and uncertainties in hillslope-scale measurements; however, these values are a reasonable first-order estimate for evaluating models. Models with watershed-scale sediment loads in the expected range were WEPP, AGWA-KINEROS2, and the VIC modules with the smallest hillslope sizes. RUSLE values were all higher than the expected SY.

Each model predicted increasing SL with larger hillslope sizes (Figures 4, S1), except for WEPP in Skin Gulch, which predicted declining SL for the watershed simulations using the largest hillslope sub-units. Even though the total watershed area was the same for all simulations, the simulated SY increased non-linearly with greater hillslope length. This effect is greatest in the hillslope version of RUSLE because it does not simulate sediment deposition within hillslopes. This scale dependence in simulated SL is not present for the gridded version of RUSLE because the L and S factors are calculated for each 30 m pixel (Winchell et al., 2008) instead of for hillslopes of varying sizes. Gridded RUSLE total SL were 112,000-155,000 Mg for Skin and Hill Gulch, respectively, at the lower range of those predicted by the hillslope version of RUSLE.

Simulated watershed-scale SL values were also sensitive to parameter selection, as shown in the VIC ensemble simulations (Figure 4, S1). Sediment loads were overall highest for VIC-HSPF and VIC-MUSLE, but VIC-DHSVM had the greatest sensitivity to parameter values, with simulated SL varying over two orders of magnitude across the ensembles of simulations for each scale of hillslope sub-units.

Table 2. Summary of watershed total sediment loads (Mg) [and sediment yields (Mg ha^{-1})] for each model and watershed divided into 0.5 ha and 25 ha target hillslope areas. RUSLE gridded values were calculated from a 30 m DEM. Values for MUSLE, HSPF, and DHSVM represent mean values calculated from ensemble simulations in VIC.

Model	**Skin**		**Hill**	
	0.5ha	*25ha*	*0.5ha*	*25ha*
RUSLE	88,000 [58]	445,000 [292]	102,000 [72]	470,000 [333]
WEPP	9,100 [6]	27,000 [16]	10,200 [7]	27,100 [19]
AGWA-KINEROS2	41,000 [27]	55,300 [36]	20,300 [14]	23,700 [17]
VIC-MUSLE	36,200 [24]	248,000 [162]	30,600 [22]	99,300 [70]
VIC-HSPF	38,700 [25]	2,470,000 [1620]	42,700 [30]	2,410,000 [1700]
VIC-DHSVM	43,400 [28]	279,000 [183]	38,100 [27]	257,000 [182]
RUSLE gridded	112,000 [73]		155,000 [110]	

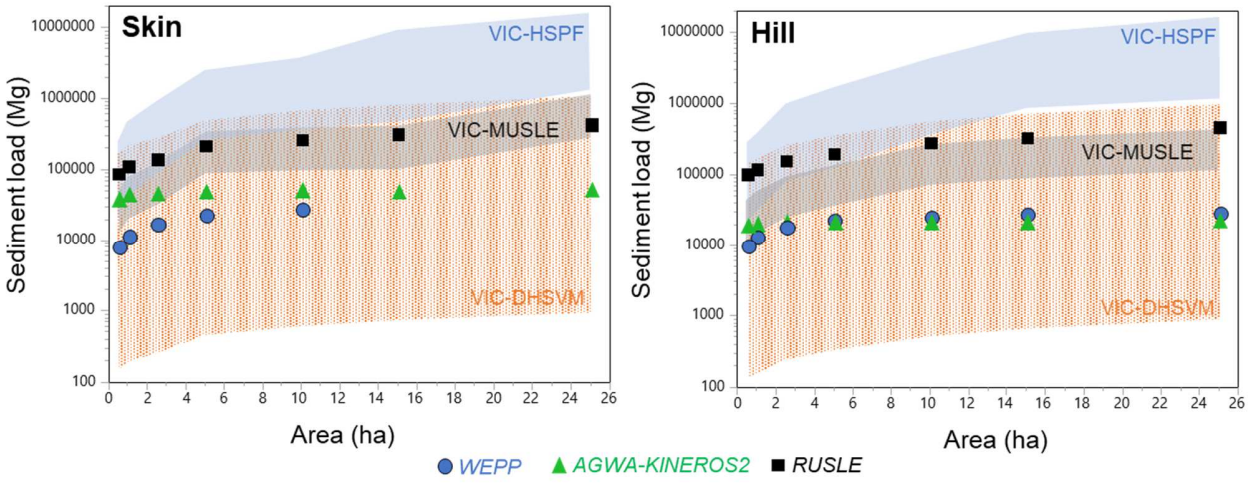

Fig. 4 Changes in simulated watershed total sediment loads with target hillslope area for Skin Gulch and Hill Gulch. Points are for WEPP, AGWA-KINEROS2, and RUSLE hillslope watershed totals, and shaded ranges are for the VIC modules with varying parameter values. Boxplots of VIC sediment loads in Figure S1. Data in Kampf et al. (2020).

Spatial patterns of SY within watersheds are shown in Figure 5. For both Skin Gulch and Hill Gulch, gridded RUSLE produced the highest SY in the center portions of the watersheds,

where burn severity was high and slopes are steep. Simulated SY rates in these areas exceeded 1,000 Mg ha^{-1} for some individual grid cells (Figure 5a). These extreme rates were less common for RUSLE applied at 2.5 ha hillslope resolution, but they were present for some hillslopes at the 25 ha resolution due to the long hillslope lengths (Figure 5b,c). WEPP simulated less spatial variability overall, but generally SY was highest in areas with high burn severity (Figure 5d,e). AGWA-KINEROS2 had isolated areas of very high erosion in both watersheds (>400 Mg ha^{-1}) with low erosion in most other locations (< 1 Mg ha^{-1}). Boundaries of the high erosion areas are similar to soil survey polygons, suggesting that this pattern relates to soil parameters.

Correlation analysis (Figure S2) indicates more similarities between models than are evident visually (Figure 5). Correlations are strongest between gridded and hillslope versions of RUSLE (r=0.69-0.81), which differed only in the original resolution of computations (Figure S2). Both versions of RUSLE were better correlated with WEPP (r=0.45-0.63; ρ=0.56-0.63) than with AGWA-KINEROS2 (r=0.01-0.26; ρ=0.22-0.50). WEPP was also significantly correlated with AGWA-KINEROS2 (r=0.58; ρ=0.63). Interestingly, the models were not consistent in simulating which of the two watersheds produced more erosion. RUSLE and WEPP simulated higher total sediment load and average sediment yield in Hill Gulch, whereas AGWA-KINEROS2, MUSLE, and DHSVM simulated higher total sediment load for Skin Gulch (Table 2). Hill Gulch has higher average hillslope lengths, slopes, and soil erodibilities, which led to higher SL in RUSLE and WEPP. In AGWA-KINEROS2, the boundaries of areas with particularly high erosion in Skin Gulch (Figure 5f,g) corresponded with boundaries of soil polygons, so these patterns were likely heavily influenced by the of soil parameter values. VIC-MUSLE, VIC-HSPF, and VIC-DHSVM had parameter values based on those in AGWA-KINEROS2, so they also produced higher SL in Skin Gulch.

The simulated patterns of relative erosion amounts (fractions of watershed total SL) for 25 ha hillslopes were significantly correlated with the fraction of total channel heads (r=0.26-0.64; ρ=0.41-0.72) (Figure 6), indicating the models all produced erosion patterns similar to those of post-fire rilling and gullying. AGWA-KINEROS2 simulations diverged most from the channel head pattern for intermediate-length hillslopes in Hill Gulch, whereas RUSLE had more outliers for the longest hillslopes in Skin Gulch because of the strong influence of length on RUSLE sediment yields.

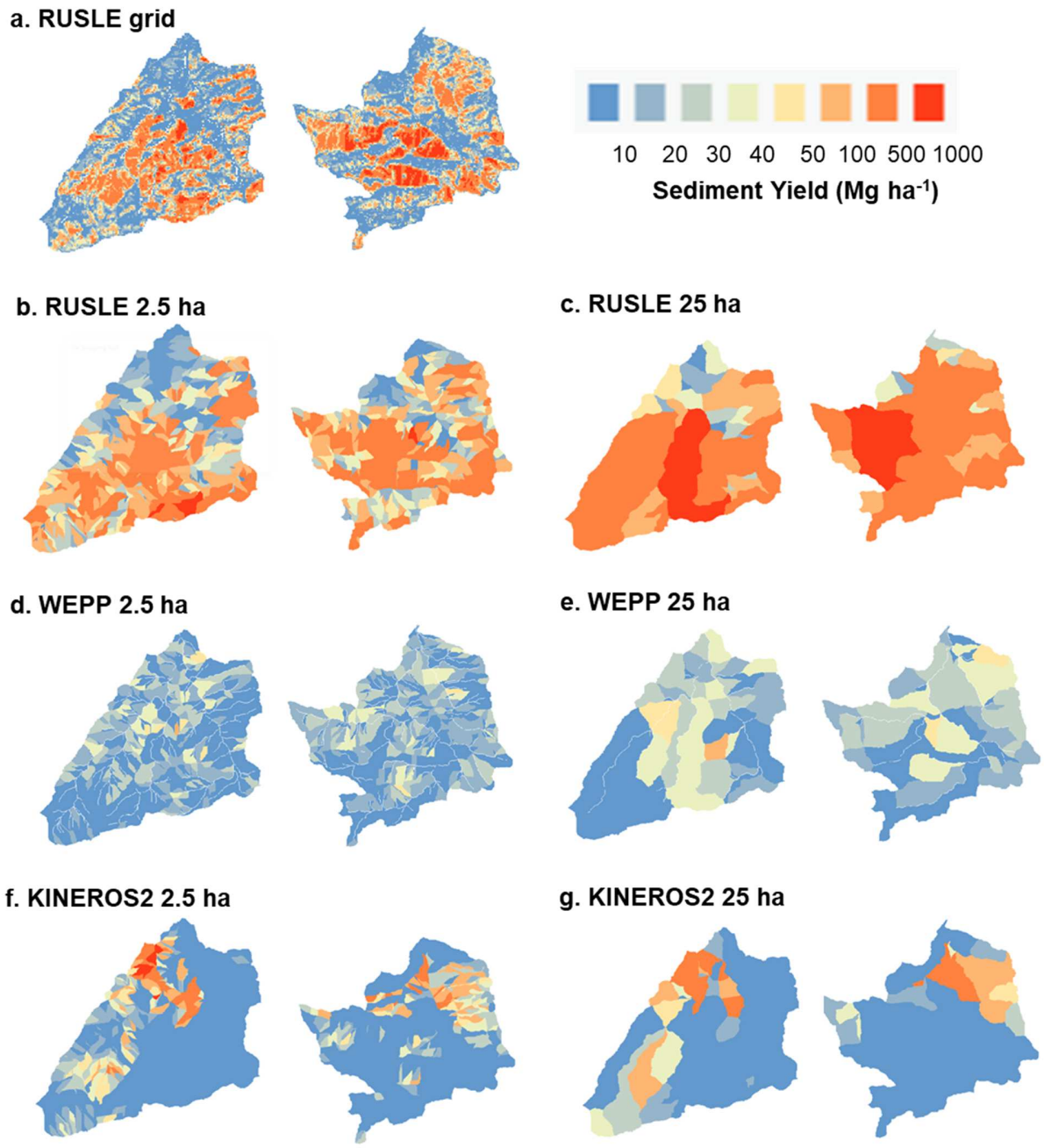

Fig. 5 Spatial patterns of simulated sediment yields (SY) for Skin Gulch (left) and Hill Gulch (right) using (a) RUSLE with values computed by 30 m grid cell; (b,c) RUSLE hillslope; (d,e) WEPP for hillslope polygons, and (f,g) AGWA-KINEROS2 for hillslope polygons. Target hillslope areas in (b,d,f) are 2.5 ha, and those for (c,e,g) are 25 ha

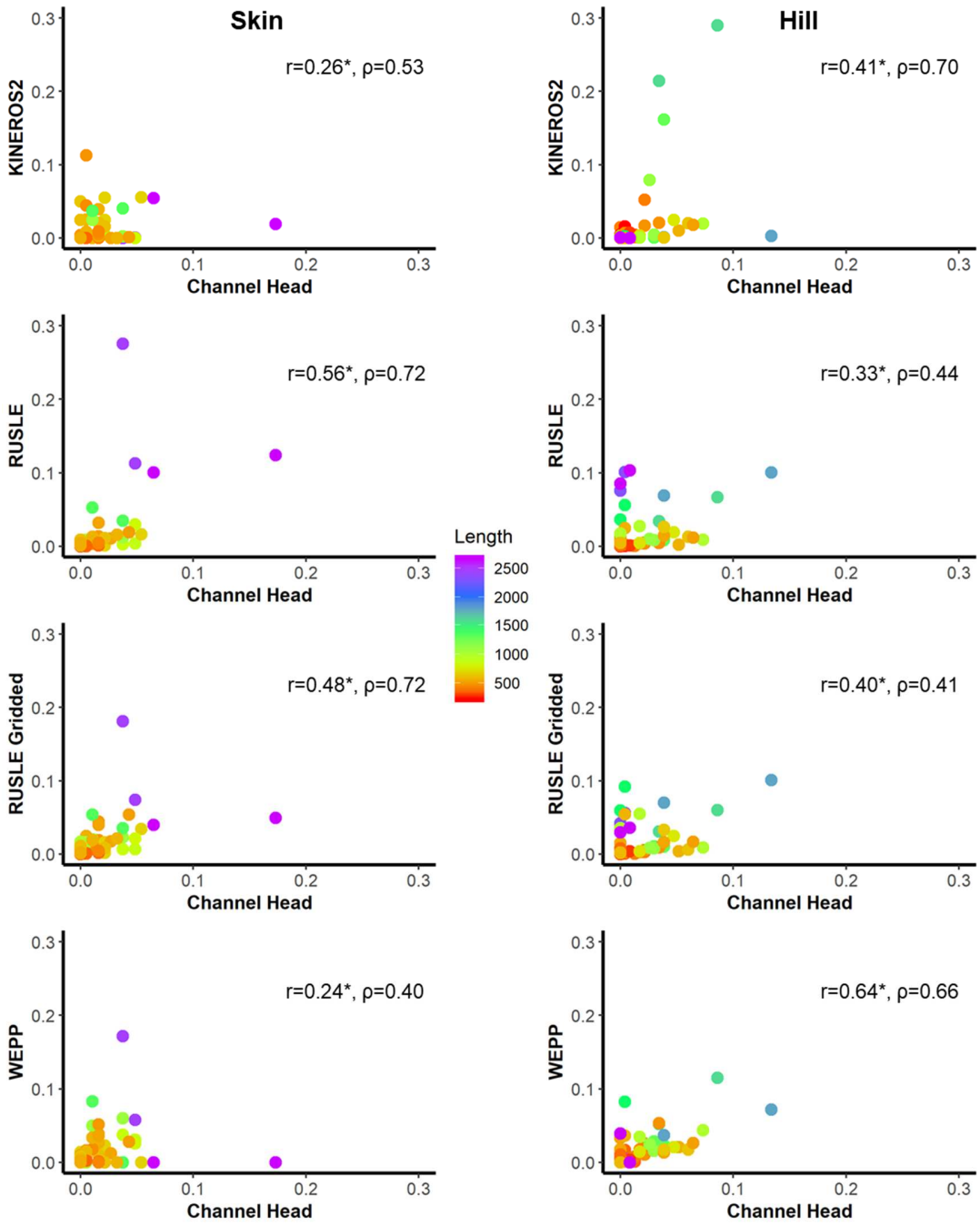

Fig. 6 Fraction of watershed total sediment load vs. fraction of watershed total channel heads by 25 ha hillslope divisions (Figure 5c,e,g). Pearson (r) and Spearman (ρ) correlation coefficients given for each combination of values; * indicates significant at $p<0.05$ Significance of ρ could not be computed due to ties. Colors of points indicate hillslope length in meters.

5. Discussion

Our results confirm prior studies showing that uncalibrated hillslope-scale erosion models are not well correlated with hillslope erosion observations (Larsen and MacDonald 2007; Miller et al. 2012). One major source of error in applying un-calibrated models to new locations is the accuracy of input parameters derived from geospatial datasets. In particular, improvements are needed in surface cover data, as bare soil is the primary variable responsible for increased post-fire erosion in Colorado (Larsen et al., 2009). Accurate representation of bare soil from satellite or airborne remote sensing data is inherently challenging because of the fine-scale heterogeneity of regrowth, but estimates could be improved with more extensive field cover measurements for training remote sensing image classifications. We recommend collecting field ground cover data where possible to support applications of erosion models for management purposes. Soil property data can also introduce error because the spatial resolution of soil survey polygons is often coarser than the size of modeled hillslopes. Many soil survey polygons contain multiple soil components, and boundaries between different surveys can cause abrupt changes in parameters. Conducting full soil surveys in new management areas is likely infeasible in most circumstances, but modelers could consider conducting sensitivity analyses, varying soil parameter values to evaluate their effects on simulated sediment yields. Finally, in the case study presented here, uncertainties in observed SY, particularly under-catch of sediment, also affected model-observation comparisons.

Although higher quality input data should improve model results, it may not be realistic to expect uncalibrated hillslope erosion models to simulate SY accurately for individual hillslopes. Each hillslope has unique and heterogeneous topography, soil, vegetation, and rainfall patterns, leading to complex internal erosion and deposition patterns that are challenging both to measure and to model. However, the reliability of these models over larger watershed areas is generally more important for management considerations, as models can guide decisions on which watersheds to target for erosion control. We found that RUSLE over-predicted erosion at the watershed scale compared to our empirical estimate, whereas WEPP and AGWA-KINEROS2 produced values that were more consistent with expected values from field observations. In part, RUSLE may overpredict because it represents gross erosion, while both erosion and deposition are modeled in WEPP and AGWA-KINEROS2. Managers should use the spatial erosion patterns simulated by these models to map areas of low and high erosion rather

than rely on the magnitudes of simulated sediment load. The relative patterns of erosion are more consistent between models than the watershed-scale sediment loads. In the watersheds evaluated here, the relative erosion patterns were significantly correlated with mapped patterns of rilling and gullying, albeit with substantial scatter in the relationships (Figure 6). This indicates that the models can identify areas that experienced high post-fire erosion, although the spatial patterns may not be entirely consistent between models.

For all models, watershed-scale sediment loads were closest to our empirical estimate when hillslopes were divided into the smallest areas (i.e., 0.5 ha). In USLE and WEPP smaller hillslopes were more realistic because the models were originally developed using plot-scale data. Relationships between simulated SY and input variables are scale-dependent in hillslope models because they use length to predict erosion rates (Wu et al., 2008; Ghaffari, 2011; Fu et al., 2015). When such models are applied to larger slopes than those for which they were developed, they may not adequately represent the erosion and deposition processes. Longer flow paths can enable greater rill and gully development, leading to concentrated flow with greater transport capacity and higher SY (Pietraszek, 2006); however, longer flow paths can also provide more opportunities for sediment to be deposited within hillslopes (Afshar et al. 2010), leading to complex and highly variable scaling relationships (Wagenbrenner and Robichaud, 2014). WEPP and AGWA-KINEROS2 allow for both erosion and deposition within hillslopes, whereas RUSLE, VIC-MUSLE, and VIC-HSPF do not. This leads to greater sensitivity to hillslope scale in the latter models. RUSLE sediment yields progressively increase with longer slopes unless a slope length threshold is applied (Nearing et al., 1990). In RUSLE, SY also increases with slope based in part on the ratio of rill to interrill erosion which increases with slope (McCool et al., 1989). Many of the study area hillslopes also had steeper slopes than were used for RUSLE development (Nearing, 1997; Renard et al., 1997). When applying these models to new watersheds that do not have erosion observations, we recommend using a fine hillslope resolution, ideally with lengths between 10-100 m, which is most comparable to the plots used to develop USLE, RUSLE, and WEPP.

An additional consideration in selecting a model is the time scale of information needed. RUSLE is intended for long time scales (seasonal, annual). WEPP simulates individual storms, but results are usually evaluated as the sums of sediment yields over seasons or years. AGWA-KINEROS2 is an event-based model that is typically applied for individual rain storms. Here we

565 compared these models in terms of their seasonal total erosion simulations to maintain
566 consistency between the three models, but further evaluation of WEPP and AGWA-KINEROS2
567 could consider simulations of individual storms. Although RUSLE does not simulate the runoff
568 response to time-varying rainfall and snowmelt; adding a runoff factor to RUSLE can improve
569 its performance (Kinnell 2010). Overall, our results demonstrate that simulations are likely to be
570 most accurate when run with fine spatial discretization (small hillslopes) and short time steps that
571 allow simulating erosion from individual storms. These finer resolution simulations aggregate to
572 more realistic sediment loads for large spatial scales (watersheds) and long time scales (seasons,
573 years).

574 ## 6. Conclusions

575 This study compared the performance of erosion models commonly used in watershed
576 management. Although most of the models were developed at hillslope scale, managers often
577 employ them for watershed scale prediction. With the exception of a site-specific regression
578 model, we found that none of the model simulations of sediment yield correlated well with SY
579 measured at hillslope sediment fences, probably due to a combination of measurement and model
580 uncertainties. RUSLE and AGWA-KINEROS2 predicted wider ranges of SY than those
581 observed in the field and substantially over-predicted some hillslope SY values, whereas WEPP
582 predicted a range of SY more consistent with field measurements. One large source of potential
583 error stems from geospatial datasets used to parameterize hillslope models; accurate maps of
584 ground cover are particularly important for erosion simulations. Given the heterogeneity of land
585 surface properties within hillslopes, it is unrealistic to expect an erosion model parameterized
586 with geospatial data to perform well for individual hillslopes. The models were somewhat more
587 consistent with one another in their simulated spatial patterns of erosion across watersheds, and
588 they all simulated erosion patterns that significantly correlated with visual observations of rill
589 and gully channel heads. This means that although the models did not capture the site-specific
590 factors that affect individual hillslopes, they were able to identify areas with high post-fire
591 erosion within watersheds, though with some variability in patterns between models.

592 The models differed more in their predictions of watershed-scale sediment loads, which
593 varied by orders of magnitude. At watershed scale, WEPP and AGWA-KINEROS2 had
594 sediment loads in the range expected from scaling up our hillslope observations, whereas

RUSLE exceeded the expected range. Departure from the expected range became greater for larger size hillslopes, so erosion models should be applied on small (<1 ha) hillslopes to avoid unrealistic increases in simulated SY caused by long slope lengths. VIC erosion model applications also highlighted substantial variability in watershed sediment loads due to parameter selection, particularly for soil parameters. Because of the high uncertainty in watershed sediment loads, users should consider making management decisions based on relative erosion patterns rather than sediment load quantities. Collecting field erosion data across multiple scales from hillslopes to watersheds is critical to future improvements in simulating watershed-scale erosion.

Acknowledgements

Post-fire erosion monitoring was funded by National Science Foundation grants [DIB-1230205] and [DIB-1339928]. Model evaluation was supported by the Colorado Water Center. Thanks to Bill Elliott and Pete Robichaud for WEPP training and theoretical background. F. Saavedra's research has been supported by Comisión Nacional de Investigación Científica y Tecnológica (CONICYT-FONDECYT) Postdoctoral [3170651] project, and C. Wilson was supported by National Science Foundation [Grant No. DGE-0966346]. Thanks to reviewers for their helpful comments. Data available in Kampf et al. (2020).

References

Afshar, F. A., Ayoubi, S., & Jalalian, A., 2010. Soil redistribution rate and its relationship with soil organic carbon and total nitrogen using 137Cs technique in a cultivated complex hillslope in western Iran. J Environ Radioact. 101(8), 606-614. https://doi.org/10.1016/j.jenvrad.2010.03.008.

Ahuja, L. R., Ii, J. A., David, O., 2005. Developing natural resource models using the object modeling system: feasibility and challenges. Adv Geosci. 4, 29-36.

Aksoy, H., Kavvas, M. L., 2005. A review of hillslope and watershed scale erosion and sediment transport models. Catena. 64(2-3), 247-271. https://doi.org/10.1016/j.catena.2005.08.008.

Baigorria, G. A., Romero, C. C., 2007. Assessment of erosion hotspots in a watershed: integrating the WEPP model and GIS in a case study in the Peruvian Andes. Environ Modell Softw. 22(8), 1175-1183. https://doi.org/10.1016/j.envsoft.2006.06.012.

Benavides-Solorio, J.D.D., MacDonald, L.H., 2005. Measurement and prediction of post-fire erosion at the hillslope scale, Colorado Front Range. Int J Wildland Fire. 14, 457–474. http://dx.doi.org/10.1071/WF05042.

Benda, L., Miller, D., Andras, K., Bigelow, P., Reeves, G, Michael, D., 2007. NetMap: a new tool in support of watershed science and resource management. Forest Science 53(2): 206–219. https://doi.org/10.1093/forestscience/53.2.206.

Bicknell, B. R., A. S. Donigian, Jr., T. H. Jobes, Chinnaswamy, R.V., 1996. Modeling Nitrogen Cycling and Export in Forested Watersheds Using HSPF. U.S. Environmental Protection Agency, National Exposure Research Laboratory, Ecosystems Research Division, Athens, Georgia, USA.

Brogan, D.J., MacDonald, L.H., Nelson, P.A., Morgan, J.A., 2019a. Geomorphic complexity and sensitivity in channels to fire and floods in mountain catchments. Geomorphology. 337, 53–68. https://doi.org/10.1016/j.geomorph.2019.03.031

Brogan, D.J., Nelson, P.A., MacDonald, L.H., 2019b. Spatial and temporal patterns of sediment storage and erosion following a wildfire and extreme flood. Earth Surf Dynam. 7, 563–590. https://doi.org/10.5194/esurf-7-563-2019

Canfield, H.E., Goodrich, D.C., 2005. Suggested changes to AGWA to account for fire (V 2.1).

643 Demaria, E.M., Nijssen, B., Wagener, T., 2007. Monte Carlo sensitivity analysis of land surface
644 parameters using the Variable Infiltration Capacity model. J Geophys Res-Atmos. 112.
645 https://doi.org/10.1029/2006JD007534
646 Desilets, S. L., Nijssen, B., Ekwurzel, B., Ferré, T. P., 2007. Post-wildfire changes in suspended
647 sediment rating curves: Sabino Canyon, Arizona. Hydrol Process. 21(11), 1413-1423.
648 https://doi.org/10.1002/hyp.6352.
649 Donigian, A.S., Love, J.T., 2003. Sediment calibration procedures and guidelines for watershed
650 modeling. Proceedings of the Water Environment Federation 2003. 728–747.
651 https://doi.org/10.2175/193864703784828345.
652 Doten, C. O., Bowling, L. C., Lanini, J. S., Maurer, E. P., Lettenmaier, D. P., 2006. A spatially
653 distributed model for the dynamic prediction of sediment erosion and transport in
654 mountainous forested watersheds. Water Resour Res. 42, W04417.
655 https://doi.org/10.1029/2004WR003829
656 Dun, S., Wu, J. Q., Elliot, W. J., Robichaud, P. R., Flanagan, D. C., Frankenberger, J. R., Brown,
657 R.E, Xu, A.C., 2009. Adapting the Water Erosion Prediction Project (WEPP) model for
658 forest applications. J Hydrol. 366(1-4), 46-54.
659 https://doi.org/10.1016/j.jhydrol.2008.12.019.
660 Eidenshink, J., Schwind, B., Brewer, K., Zhu, Z. L., Quayle, B., Howard, S., 2007. A project for
661 monitoring trends in burn severity. Fire Ecol. 3(1), 3-21.
662 https://doi.org/10.4996/fireecology.0301003.
663 Elliot, W. J., 2004. WEPP internet interfaces for forest erosion prediction. J Am Water Resour
664 As. 40(2), 299-309. https://doi.org/10.1111/j.1752-1688.2004.tb01030.x.
665 Elliot, W. J., Miller, M. E., Enstice, N., 2016. Targeting forest management through fire and
666 erosion modelling. Int J Wildland Fire. 25(8), 876-887.
667 https://doi.org/10.1071/WF15007.
668 Flanagan,D.C., Nearing, M.A., 1995. Water Erosion Prediction Project Hillslope Profile and
669 Watershed Model Documentation.NSERL Report No.10,West Lafayette,IN: National
670 Soil Erosion Research Laboratory
671 Frankenberger, J. R., Dun, S., Flanagan, D. C., Wu, J. Q., Elliot, W. J., 2011. Development of a
672 GIS interface for WEPP model application to Great Lakes forested watersheds. In ISELE

673 Paper Number 11139. Paper presented at the international symposium on erosion and
674 landscape evolution; September 18-21, 2011; Anchorage, AK. 8 p.
675 Fu, B. J., Zhao, W. W., Chen, L. D., Zhang, Q. J., Lü, Y. H., Gulinck, H., Poesen, J., 2005.
676 Assessment of soil erosion at large watershed scale using RUSLE and GIS: a case study
677 in the Loess Plateau of China. Land Degrad Dev. 16(1), 73-85.
678 https://doi.org/10.1002/ldr.646.
679 Fu, S., Cao, L., Liu, B., Wu, Z., Savabi, M. R., 2015. Effects of DEM grid size on predicting soil
680 loss from small watersheds in China. Environ Earth Sci. 73(5), 2141-2151.
681 https://doi.org/10.1007/s12665-014-3564-3.
682 Gannon, B. M., Wei, Y., MacDonald L.H., Kampf, S.K., Jones, K.W., Cannon, J.B., Wolk, B.H.,
683 Cheng, A.S., Addington R.N., Thompson, M.P., 2019. Prioritising fuels reduction for
684 water supply protection. Int J Wildland Fire. 28, 785-803.
685 https://doi.org/10.1071/WF18182.
686 Garbrecht, J., Martz, L. W., 1997. The assignment of drainage direction over flat surfaces in
687 raster digital elevation models. J Hydrol. 193(1-4), 204-213.
688 https://doi.org/10.1016/S0022-1694(96)03138-1.
689 Ghaffari, G., 2011. The impact of DEM resolution on runoff and sediment modelling results. Res
690 J Environ Sci. 5(8), 691-702.
691 Goodrich, D. C., Burns, I. S., Unkrich, C. L., Semmens, D. J., Guertin, D. P., Hernandez, M.,
692 Yatheendradas, S., Kennedy, J.R., Levick, L. R., 2012. KINEROS2/AGWA: model use,
693 calibration, and validation. T ASABE. 55(4), 1561-1574.
694 Henkle, J. E., Wohl, E., & Beckman, N. (2011). Locations of channel heads in the semiarid
695 Colorado Front Range, USA. Geomorphology, 129(3-4), 309-319.
696 https://doi.org/10.1016/j.geomorph.2011.02.026.
697 Johnson, R. C., Imhoff, J. C., & Davis, H. H. (1980). User's Manual of the Hydrologie
698 Simulation Program-FORTRAN (HSPF). US Environmental Protection Agency, Athens,
699 GA. EPA-600/9/80-015.
700 Jones, K. W., Cannon, J. B., Saavedra, F. A., Kampf, S. K., Addington, R. N., Cheng, A. S.,
701 MacDonald, L.H., Wilson, C.,Wolk, B., 2017. Return on investment from fuel treatments
702 to reduce severe wildfire and erosion in a watershed investment program in Colorado. J
703 Environ Manage. 198, 66-77. https://doi.org/10.1016/j.jenvman.2017.05.023.

Kampf, S. K., Brogan, D. J., Schmeer, S., MacDonald, L. H., Nelson, P. A., 2016. How do geomorphic effects of rainfall vary with storm type and spatial scale in a post-fire landscape?. Geomorphology. 273, 39-51. https://doi.org/10.1016/j.geomorph.2016.08.001.

Kampf, S., Schmeer, S., MacDonald, L., Gannon, B., Saavedra, F., Miller, M.E., Heldmeyer, A., Livneh, B. 2020. High Park Fire hillslope erosion data and watershed simulations, HydroShare, https://doi.org/10.4211/hs.b3ca27267d0c4a23b7f459917e3067ec

Kinnell, P. I. A., 2010. Event soil loss, runoff and the Universal Soil Loss Equation family of models: A review. J Hydrol. 385(1-4), 384-397. https://doi.org/10.1016/j.jhydrol.2010.01.024.

Kunze, M. D., Stednick, J. D., 2006. Streamflow and suspended sediment yield following the 2000 Bobcat fire, Colorado. Hydrol Process. 20(8), 1661-1681. https://doi.org/10.1002/hyp.5954.

Laflen, J. M., Flanagan, D. C., 2013. The development of US soil erosion prediction and modeling. International Soil and Water Conservation Research. 1(2), 1-11. https://doi.org/10.1016/S2095-6339(15)30034-4.

Laflen, J.M., Elliot, W.J., Simanton, R., Holzhey, S., Kohl, K.D., 1991. WEPP soil erodibility experiments for rangeland and cropland soils. J Soil Water Conserv. 46(1), 39-44.

Larsen, I. J., MacDonald, L. H., 2007. Predicting postfire sediment yields at the hillslope scale: Testing RUSLE and Disturbed WEPP. Water Resour Res. 43(11). https://doi.org/10.1029/2006WR005560.

Larsen, I.J., MacDonald, L.H., Brown, E., Rough, D., Welsh, M.J., Pietraszek, J.H., Libohova, Z., Benavides-Solorio, J.D., Schaffrath, K., 2009. Causes of post-fire runoff and erosion: water repellency, cover, or soil sealing? Soil Sci Soc Am J. 73, 1393-1407. https://doi.org/10.2136/sssaj2007.0432

Liang, X., Lettenmaier, D. P., Wood, E. F., Burges, S. J., 1994. A simple hydrologically based model of land surface water and energy fluxes for general circulation models. J Geophys Res-Atmos. 99(D7), 14415-14428. https://doi.org/10.1029/94JD00483.

Litschert, S.E., Theobald, D.M., Brown, T.C., 2014. Effects of climate change and wildfire on soil loss in the Southern Rockies Ecoregion. Catena. 118, 206-219. http://dx.doi.org/10.1016/j.catena.2014.01.007

735 Livneh, B., Bohn, T.J., Pierce, D.W., Munoz-Arriola, F., Nijssen, B., Vose, R., Cayan, D.R.,
736 Brekke, L., 2015. A spatially comprehensive, hydrometeorological data set for Mexico,
737 the U.S., and Southern Canada 1950–2013. Sci Data. 2, 150042.
738 https://doi.org/10.1038/sdata.2015.42
739 Livneh, B., Rosenberg, E.A., Lin, C., Nijssen, B., Mishra, V., Andreadis, K.M., Maurer, E.P.,
740 Lettenmaier, D.P., 2013. A Long-Term Hydrologically Based Dataset of Land Surface
741 Fluxes and States for the Conterminous United States: Update and Extensions. J Climate.
742 26, 9384–9392. https://doi.org/10.1175/JCLI-D-12-00508.1
743 Maidment, D.R., 1993. Handbook of Hydrology. McGraw-Hill, New York.
744 McCool, D.K., Foster, G.R., Mutchler, C.K., Meyer, L.D., 1989. Revised slope length factor for
745 the Universal Soil Loss Equation. T ASAE. 32, 1571–1576.
746 https://doi.org/10.13031/2013.31192
747 Merritt, W. S., Letcher, R. A., Jakeman, A. J., 2003. A review of erosion and sediment transport
748 models. Environ Modell Softw. 18(8-9), 761-799. https://doi.org/10.1016/S1364-
749 8152(03)00078-1.
750 Miller, J. D., Nyhan, J. W., Yool, S. R., 2003. Modeling potential erosion due to the Cerro
751 Grande Fire with a GIS-based implementation of the Revised Universal Soil Loss
752 Equation. Int J Wildland Fire. 12(1), 85-100. https://doi.org/10.1071/WF02017.
753 Miller, M. E., MacDonald, L. H., Robichaud, P. R., Elliot, W. J., 2012. Predicting post-fire
754 hillslope erosion in forest lands of the western United States. Int J Wildland Fire. 20(8),
755 982-999. https://doi.org/10.1071/WF09142.
756 Miller, M.E., Elliot, W.J., Billmire, M., Robichaud, P.R., Endsley, K.A., 2016. Rapid-response
757 tools and datasets for post-fire remediation: linking remote sensing and process-based
758 hydrological models. Int J Wildland Fire. 25(10), 1061-1073.
759 https://doi.org/10.1071/WF15162.
760 Miller, S. N., Semmens, D. J., Goodrich, D. C., Hernandez, M., Miller, R. C., Kepner, W. G.,
761 Guertin, D. P., 2007. The automated geospatial watershed assessment tool. J Environ
762 Modeling and Software. 22(3), 365-377. https://doi.org/10.1016/j.envsoft.2005.12.004.
763 Miller, S., Rhodes, C., Robichaud, P., Ryan, S., Kovecses, J., Chambers, C., Rathburn, S., Heath,
764 J., Kampf, S., Wilson, C., Brogan, D. Piehl, B., Miller, M.E., Giordanengo, J., Berryman,
765 E., Rocca, M., 2017. Learn from the burn: the High Park Fire 5 years later. Science You

766 Can Use Bulletin, Issue 25. Fort Collins, CO: Rocky Mountain Research Station. 18 p.,
767 18.
768 Millward, A. A., Mersey, J. E., 1999. Adapting the RUSLE to model soil erosion potential in a
769 mountainous tropical watershed. Catena. 38(2), 109-129. https://doi.org/10.1016/S0341-
770 8162(99)00067-3.
771 Nearing, M. A., 1997. A single, continuous function for slope steepness influence on soil loss.
772 Soil Sci Soc Am J. 61(3), 917-919.
773 https://doi.org/10.2136/sssaj1997.03615995006100030029x.
774 Nearing, M. A., Deer-Ascough, L., Laflen, J. M., 1990. Sensitivity analysis of the WEPP
775 hillslope profile erosion model. T ASAE. 33(3), 839-0849.
776 Pietraszek, J.H., 2006. Controls on Post-fire Erosion at the Hillslope Scale, Master's Thesis.
777 Colorado State University: Fort Collins, CO; 124 pp.
778 Renard, K. G., Foster, G.R., Weesies, G.A., McCool, D. K., Yoder, D.C., 1997. Predicting soil
779 erosion by water: A guide to conservation planning with the Revised Universal Soil Loss
780 Equation (RUSLE). Agricultural Handbook No.703.U. S. Dept. of Agr.: Washington DC.
781 384 pp.
782 Renschler, C.S., 2003. Designing geo-spatial interfaces to scale process models: The GeoWEPP
783 approach. Hydrol Process. 17, 1005-1017. https://doi.org/10.1002/hyp.1177.
784 Robichaud, P. R., Elliot, W. J., Pierson, F. B., Hall, D. E., & Moffet, C. A. (2007). Predicting
785 postfire erosion and mitigation effectiveness with a web-based probabilistic erosion
786 model. Catena, 71(2), 229-241. https://doi.org/10.1016/j.catena.2007.03.003.
787 Robichaud, P. R., Elliot, W. J., Lewis, S. A., Miller, M. E., 2016. Validation of a probabilistic
788 post-fire erosion model. Int J Wildland Fire. 25(3), 337-350.
789 https://doi.org/10.1071/WF14171.
790 Schmeer, S. R., Kampf, S. K., MacDonald, L. H., Hewitt, J., Wilson, C., 2018. Empirical models
791 of annual post-fire erosion on mulched and unmulched hillslopes. Catena. 163, 276-287.
792 https://doi.org/10.1016/j.catena.2017.12.029.
793 Schmeer, S.R., 2014. Post-fire Erosion Response and Recovery, High Park Fire, Colorado (M.S.
794 Thesis). Colorado State University.
795 Sharp, R., Tallis, H.T., Ricketts, T., Guerry, A.D., Wood, S.A., Chaplin-Kramer, R., Nelson, E.,
796 Ennaanay, D., Wolny, S., Olwero, N., Vigerstol, K., Pennington, D., Mendoza, G.,

797 Aukema, J., Foster, J., Forrest, J., Cameron, D., Arkema, K., Lonsdorf, E., Kennedy, C.,
798 Verutes, G., Kim, C.K., Guannel, G., Papenfus, M., Toft, J., Marsik, M., Bernhardt, J.,
799 Griffin, R., Glowinski, K., Chaumont, N., Perelman, A., Lacayo, M. Mandle, L., Hamel,
800 P., Vogl, A.L., Rogers, L., Bierbower, W., Denu, D., Douglass, J., 2018. InVEST
801 3.6.0.post62+ug.h3ee8dba1d711 User's Guide. The Natural Capital Project, Stanford
802 University, University of Minnesota, The Nature Conservancy, and World Wildlife Fund.
803 Shen, Z. Y., Gong, Y. W., Li, Y. H., Hong, Q., Xu, L., Liu, R. M., 2009. A comparison of WEPP
804 and SWAT for modeling soil erosion of the Zhangjiachong Watershed in the Three
805 Gorges Reservoir Area. Agr Water Manage. 96(10), 1435-1442.
806 https://doi.org/10.1016/j.agwat.2009.04.017.
807 Smith, R. E., Goodrich, D. C., Woolhiser, D. A., Unkrich, C. L., 1995. Chapter 20: KINEROS:
808 A kinematic runoff and erosion model, in: Singh, V.J. (Ed.), In Computer Models of
809 Watershed Hydrology, Water Resources Publications, Highlands Ranch, pp. 697-732.
810 Soil Survey Staff, Natural Resources Conservation Service, United States Department of
811 Agriculture. Soil Survey Geographic (SSURGO) Database. Available online at
812 https://sdmdataaccess.sc.egov.usda.gov. Accessed 2014.
813 Soil Survey Staff, Natural Resources Conservation Service, United States Department of
814 Agriculture. U.S. General Soil Map (STATSGO2). Available online at
815 https://sdmdataaccess.sc.egov.usda.gov. Accessed 2014.
816 Srivastava, A., Wu, J. Q., Elliot, W. J., Brooks, E. S., Flanagan, D. C., 2018. A Simulation Study
817 to Estimate Effects of Wildfire and Forest Management on Hydrology and Sediment in a
818 Forested Watershed, Northwestern US. T ASABE. 61(5), 1579-1601.
819 Stewart, J. R., Livneh, B., Kasprzyk, J. R., Rajagopalan, B., Minear, J. T., Raseman, W. J., 2017.
820 A multialgorithm approach to land surface modeling of suspended sediment in the
821 Colorado Front Range. J Adv Model Earth Sy. 9(7), 2526-2544.
822 https://doi.org/10.1002/2017MS001120.
823 Theobald, D.M., Merritt, D.M., Norman, J.B. III., 2010. Assessment of threats to riparian
824 ecosystems in the western U.S.: a report presented to the Western Environmental Threats
825 Assessment Center, Prineville, OR by the U.S.D.A., Stream Systems Technology Center
826 and Colorado State University, Fort Collins, 61p.

827 Troy, T.J., Wood, E.F., Sheffield, J., 2008. An efficient calibration method for continental-scale
828 land surface modeling. Water Resour Res. 44. https://doi.org/10.1029/2007WR006513
829 Wagenbrenner, J. W., Robichaud, P. R., 2014. Post-fire bedload sediment delivery across spatial
830 scales in the interior western United States. Earth Surf Proc Land. 39(7), 865-876.
831 Wicks, J.M., Bathurst, J.C., 1996. SHESED: a physically based, distributed erosion and sediment
832 yield component for the SHE hydrological modelling system. J Hydrol. 175, 213–238.
833 https://doi.org/10.1016/S0022-1694(96)80012-6
834 Wigmosta, M.S., Vail, L.W., Lettenmaier, D.P., 1994. A distributed hydrology-vegetation model
835 for complex terrain. Water Resour Res. 30, 1665–1679.
836 https://doi.org/10.1029/94WR00436
837 Williams, J. R., 1975. Sediment yield predictions with universal equation using runoff energy
838 factor. In:Present and Prospective Technology for Predicting Sediment Yields and
839 Sources. ARS-S-40 Agr. Res. Serv.,U.S.Dept. Agr. Washington,D.C. pp.244-252.
840 Williams, J.R., Berndt, H.D., 1977. Sediment yield prediction based on watershed hydrology. T
841 ASAE. 20(6), 1100-1104.
842 Wilson, C., 2019. The frequency, magnitude and connectivity of post-wildfire rainfall-runoff and
843 sediment transport. PhD Dissertation, Colorado State University.
844 Winchell, M.F., Jackson, S.H., Wadley, A.M., Srinivasan, R., 2008. Extension and validation of
845 a geographic information system-based method for calculating the Revised Universal Soil
846 Loss Equation length-slope factor for erosion risk assessments in large watersheds. J Soil
847 Water Conserv. 63, 105–111. https://doi.org/10.2489/JSWC.63.3.105
848 Wischmeier,W. H., Smith, D.D., 1965. Predicting rainfall-erosion losses from cropland east of
849 the Rocky Mountains,Guide forselection of practices for soil and water conservation.
850 Agriculture Handbook No. 282. Agricultural Research Service,U. S. Dept.of Agric.:
851 Washington DC. 47 pp.
852 Wohl, E., 2013. Migration of channel heads following wildfire in the Colorado Front Range,
853 USA. Earth Surf Proc Land. 38(9), 1049-1053. https://doi.org/10.1002/esp.3429.
854 Woolhiser, D. A., Smith, R. E., Goodrich, D. C., 1990. KINEROS, A Kinematic Runoff and
855 Erosion Model: Documentation and User Manual. ARS-77. Tucson, Ariz.: USDA-ARS
856 Southwest Watershed Research Center. Available at: www.tucson.ars.ag.gov/kineros.

Wu, S., Li, J., Huang, G. H., 2008. A study on DEM-derived primary topographic attributes for hydrologic applications: Sensitivity to elevation data resolution. Appl Geogr. 28(3), 210-223. https://doi.org/10.1016/j.apgeog.2008.02.006.

Yanto, Livneh, B., Rajagopalan, B., Kasprzyk, J., 2017. Hydrological model application under data scarcity for multiple watersheds, Java Island, Indonesia. J Hydrol: Regional Studies. 9, 127–139. https://doi.org/10.1016/j.ejrh.2016.09.007

Yochum, S.E., Norman, J., 2014. West Fork Complex Fire: potential increase in flooding and erosion. U.S.D.A. Natural Resources Conservation Service Report, Colorado, 32 p.

Yochum, S.E., Norman, J.B., 2015. Wildfire-induced flooding and erosion-potential modeling: examples from Colorado, 2012 and 2013. Proceedings of the 3rd Joint Federal Interagency Conference on Sedimentation and Hydrologic Modeling, April 19-23, 2015, Reno, Nevada, USA, 953-964. https://doi.org/10.13140/RG.2.1.4422.1923.